Multi-Scale Modeling of Wetting: Effects of Surface Roughness

Conference Paper · November 2014

CITATIONS
2

READS
1,565

6 authors, including:

Ronaldo Giro
IBM
59 PUBLICATIONS **709** CITATIONS
SEE PROFILE

Peter W Bryant
Jacksonville State University
38 PUBLICATIONS **72** CITATIONS
SEE PROFILE

Rafael Rodrigues Del Grande
University of California, Merced
12 PUBLICATIONS **90** CITATIONS
SEE PROFILE

Claudius Feger
IBM
64 PUBLICATIONS **1,440** CITATIONS
SEE PROFILE

MULTI-SCALE MODELING OF WETTING: EFFECTS OF SURFACE ROUGHNESS

Ronaldo Giro

Peter W. Bryant

Mathias B. Steiner

Rafael R. Del Grande

Claudius Feger

rgiro@br.ibm.com

pbryant@br.ibm.com

msteine@us.ibm.com

rdgrande@br.ibm.com

feger@us.ibm.com

IBM Research Brazil

Av. Pasteur 138/146 - Botafogo - Rio de Janeiro - RJ, CEP 22290-240, Brazil

Michael Engel

engelm@us.ibm.com

T. J. Watson Research Center

1101 Kitchawan Rd, Ossining, NY 10598, United States

Abstract. *Contact angle is the angle at which the liquid-vapor interface meets the solid-liquid interface. As the tendency of a drop to spread out over a flat, solid surface increases, the contact angle decreases. Thus the contact angle provides an inverse measure of wettability. Although it is relatively easy to measure the contact angle in the macroscopic domain, it is very difficult to obtain the intrinsic wettability of a surface. When measuring the contact angle, we obtain the apparent contact angle, which depends collectively on surface roughness and chemical contaminants on the surface. In order to relate the intrinsic contact angle with the apparent one, we have developed a multi-scale approach. From Classical Molecular Dynamics (from the microscopic domain) the intrinsic contact angle is obtained. The Lattice Boltzmann Method (mesoscale simulation) incorporates the effects of surface roughness, surface curvature and the size of the drop to obtain the apparent (macroscopic) contact angle. We employ this approach*

for a case study of a decane oil drop immersed in water over a quartz surface and a glass surface.

Keywords: *Wettability, Contact Angle, Molecular Dynamics Simulations, Lattice Boltzmann Simulations*

1 INTRODUCTION

Wettability is a topic of great interest because of the challenge of understanding the phenomenon scientifically and the wide variety of technological and industrial applications it affects. Some examples of applications affected by wetting phenomena are self-cleaning surfaces (Ma and Hill, 2006), oil extraction from porous rock (Zhang et al., 2006), froth flotation (Fuerstenau et al., 2007) or acid heap leaching (von Michaelis, 1989) in mineral recovery, and various other industrial applications (de Gennes et al., 2004; Starov et al., 2007), e.g., protective spin coating of surfaces (CDs, DVDs, glass lenses, car mirrors and windows), and ink-jet printing.

In a general sense, wettability measures the affinity of one particular liquid for a solid surface. Frequently, wettability is quantified by using the definition of the contact angle. The contact angle is the angle at which the liquid-vapor interface meets the solid-liquid interface. As the tendency of a drop to spread out over a flat, solid surface increases, the contact angle decreases. The contact angle therefore provides an inverse measure of wettability. Although it is relatively easy to measure the contact angle in the macroscopic domain, it is very difficult to obtain the intrinsic wettability of a surface. When measuring the contact angle, one obtains the apparent contact angle. The interpretation of this observed, apparent contact angle is complicated by many factors such as surface roughness, chemical contaminants, heterogeneity of the system, presence of surfactants, and line tension (Amirfazlia and Neumann, 2004). Complications specific to surface roughness include (Wolf et al., 2009): (i) the apparent contact angle (based on the average plane of the surface) can differ markedly from the intrinsic contact angle, which is based on the local orientation of the surface; (ii) drops with differing initial conditions show different contact angles due to hysteresis effects; and finally (iii) scale effects - with increasing drop size, the effect of roughness decreases, and the static apparent contact angle approaches the intrinsic angle.

Line tension (Amirfazlia and Neumann, 2004) is localized at the so-called three phase line where three interfaces meet, i.e., the periphery of the contact circle of a liquid drop that is placed on a solid surface and is surrounded by a vapor or other immiscible liquid phase (see Fig. 1). The concept of line tension is similar to that of surface tension. The cohesive forces between the molecules are responsible for both. In the bulk of a liquid/solid, each molecule/atom is pulled equally in every direction by neighboring molecules/atoms, resulting in a net force of zero. The molecules/atoms at the surface or at the three-phase confluence zone, do not have other molecules/atoms on all sides of them and therefore experience a net force. This force acting at a surface is called the surface tension. When it acts at the three-phase confluence zone, it is called the line tension. Line tension can modify the contact angle when the curvature radius of a drop or of a surface is small enough (less than hundreds of nanometers), and its effect is significant at the molecular scale (Amirfazlia and Neumann, 2004).

In this work we focus on surface roughness and line tension. To isolate these effects and at the same time obtain the intrinsic contact angle and the influence of line tension, we use a multi-scale, bottom-up modeling approach. Using Classical Molecular Dynamics (CMD) simulations in the microscopic domain the intrinsic contact angle is obtained, and the influence of line tension is analyzed. Lattice Boltzmann Method (LBM) is used to study the effects of surface roughness, surface curvature and the size of the drop on the apparent contact angle. The intrinsic contact angle obtained from CMD is used to tune the potential interaction between the two fluids and between the fluids and the solid in LBM. And finally, a glass surface topography

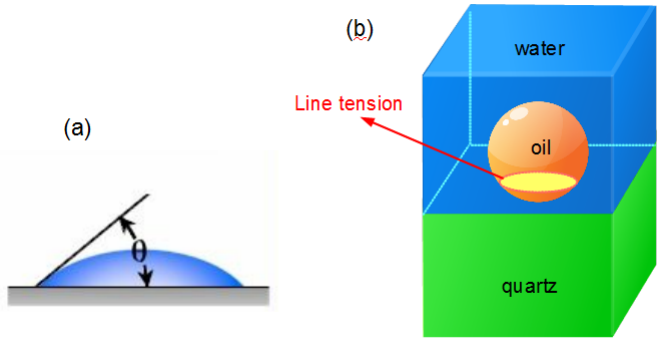

Figure 1: Schematic representation of (a) contact angle θ, and (b) the three phase line.

obtained from Atomic Force Microscopy is used to create the surface in an LBM simulation of the coupled effects of roughness and drop size. In the next sections we will show the results of this approach.

2 MOLECULAR MODELING OF INTRINSIC CONTACT ANGLE

2.1 Decane drop on a quartz surface surrounded by water

To study the contact angle between quartz, decane and water we used a slab of α-quartz ((100) direction) built from an α-quartz unit cell to a 28x34x6 supercell. A set of cubic boxes containing decane molecules surrounded by water molecules was placed on the hydroxyl group passivated α-quartz slab. The dimension of the set of cubic boxes containing decane molecules covers 4 nm, 5 nm, 6 nm, 7 nm and 9 nm. The dimension of the simulation box for the system quartz, decane and water is L_x = 15.1 nm and L_y = 16.6 nm. We used L_z = 13.5 nm for simulation boxes containing decane cubic box dimension of 4 to 6 nm. For those with decane cubic box with dimension 7 and 9 nm, we used L_z = 15.6 nm and 17.5 nm, respectively. These L_z dimensions were used in order to keep a water slab of at least 5 nm above the cubic box containing decane molecules.

In CMD simulations the interactions between atoms are modeled using a classical force field. For decane, CHARMM-based force field (Brooks, 2009) parameters were used, and for water, SPCE/FH potentials (Alejandre et al., 2009) were used. For the hydroxylated quartz we used the CWCA force field (Cruz-Chu et al., 2006). For long-range electrostatic interactions, the reciprocal space particle particle particle-mesh (PPPM) method (Hockney and Eastwood, 1989) was adopted. For all calculations we used a time step of 0.5 fs, a cutoff radius of 10 Å for van der Waals interactions, a temperature of 300 K and a pressure of 1 atm. The environmental conditions of temperature and pressure were chosen in order to compare the simulations with experimental results, which are conducted at such conditions. Other conditions of temperature and pressure are easily implemented, if needed. To control the temperature and pressure, Nosé-Hoover thermostats and barostats were used with a relaxation time of 0.1 ps and 1 ps, respectively. In order to get the equilibrium density of the fluid at a specific temperature and pressure, the following protocol was employed: First a 1 ps run was performed for the NVE ensemble (micro canonical ensemble - constant number of atoms, volume and energy), followed by 10 ps for the NVT ensemble (canonical ensemble - constant number of atoms, volume and

temperature), and finally 2 ns for the NPT ensemble (isothermal-isobaric or grand canonical ensemble - constant number of atoms, pressure and temperature). During this equilibration procedure, periodic boundary conditions were used in all three dimensions (x, y and z directions). Once the system was equilibrated, 2 ns more of NVT production simulation was performed. During this stage, periodic boundary conditions were used along only the x- and y-directions. A purely reflecting wall was placed at the top of the simulation cell to prevent the escape of water and decane molecules. This arrangement in the simulation cell was expected to diminish the boundary effect along the z-direction. All CMD simulations were performed with the LAMMPS package (Plimpton, 1995).

During the computing production stage the trajectories (atom positions) were collected at each 0.5 ps, and then the decane drop profile was obtained as the time averaged positions of the decane carbon atoms at the drop interface with water. By fitting an analytical function to the decane drop profile, the contact angle was obtained.

It is well known that the choice of fitting function can affect the value of contact angle. In the literature, usually two different approaches are taken once the bondary has been identified. (Werder et al., 2003) employs a circular best fit to estimate the contact angle. In contrast, (Giovambattista et al., 2007) makes no geometrical assumptions about the drop profile, and fits the boundary data with the function $f(z) = Az^2 + Bz + C$ where z is the distance of a water molecule from the surface. (Sergi et al., 2012) compare the circular fitting with the piecewise linear fitting and concluded that piecewise linear fitting is more precise than circular fitting. We have tried to fit a circular function, but the cubic polynomial fitting appears to be more precise due to the following reasons: (i) it captures the drop curvature near the three phase contact line, and (ii) even for the largest drops, the profile still deviates from a perfectly spherical cap (Sergi et al., 2012).

In Fig. 2 (a) we show the results of CMD simulations for a 8 nm diameter decane drop surrounded by water on a quartz surface. In (b) we show the corresponding drop profile. In that plot, z is the drop height, and r is the distance of drop interface from the z axis. The z axis passes through the center of mass of the decane drop, so if the drop has a spherical shape, the z axis is an axis of symmetry. By fitting a cubic polynomial to the data points obtained from CMD simulations (represented by the points in Fig. 2 (b)) we can obtain the contact angle. For this case we obtained a contact angle of 123.7° corresponding to the microscopic contact angle, which is different from the macroscopic contact angle because of line tension effects. In very small drop sizes the line tension has considerable effect and dramatically affects the value of the contact angle.

To evaluate the effect of line tension on the microscopic contact angle, the following procedure was adopted. By varying the size of the decane drop and plotting the cosine of the microscopic contact angle, θ, versus the inverse of the base radius, r_B, of the drop, we obtain the macroscopic contact angle, θ_∞, as a linear fit of data points extrapolated to infinity ($r_B \to \infty$). With this procedure and using the modified Young equation (Eq. 1) (Abraham and Ko, 1989; Amirfazlia and Neumann, 2004; Widom, 1995), we can obtain the macroscopic contact angle on a controlled surface and, at the same time, the line tension σ.

$$\cos(\theta) = \cos(\theta_\infty) - \frac{\sigma}{r_B \gamma_{wo}} \tag{1}$$

In the above equation, γ_{wo} is the surface tension between water and decane.

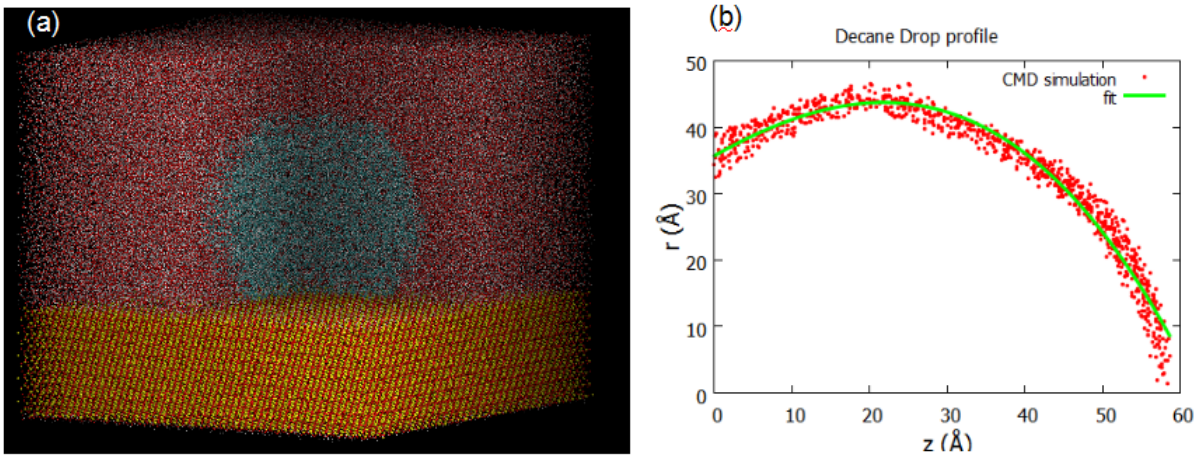

Figure 2: (a) Schematic representation of a 8 nm diameter decane drop on a quartz surface surrounded by water; (b) 8 nm diameter decane drop profile. Points represent the time averaged positions of the interfacial carbons atoms obtained from CMD simulations; the line is the cubic polynomial fit ($-0.000153z^3 - 0.0102z^2 + 0.6622z + 35.7$)**.**

The results of this procedure are shown in Fig. 3. The microscopic contact angles obtained from CMD simulations (points in Fig. 3) show the importance of line tension for microscopic scales. As the decane drop size decreases, the microscopic contact angle increases. The cosine of the contact angle is well approximated as a quadratic polynomial function (ax^2+bx+c) of the inverse of the drop base radius, as can be seen from the fitted curve. The polynomial coefficients obtained through the least square fit are: a = (201 $\pm$ 30) Å^2, b = (–25 $\pm$ 2) Å, and c = –0.01 $\pm$ 0.04. Although the expected result was a linear function, as indicated by the Modified Young Equation (Eq. 1), the quadratic polynomial function is not surprising. Amirfazlia and Neumann (2004) stated that sometimes an additional term on the right-hand side of Eq. 1 is necessary to account for high curvature situations, e.g., small thin films or microscopic systems/drops.

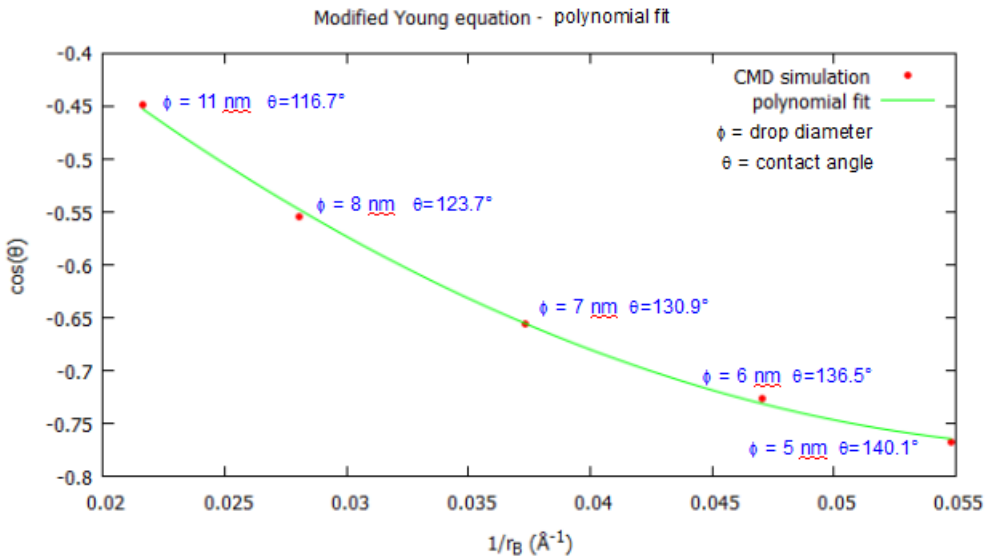

Figure 3: Cosine of contact angle versus the inverse of the drop base radius. Points represent the microscopic contact angle obtained with CMD simulations (see text for details); the line is a quadratic polynomial fit to the data.

In this work our focus is on the last two terms of the obtained quadratic polynomial fit, $ax^2 + bx + c$, i.e, the linear term $bx + c$ (first order correction of the contact angle). From coefficient b we obtain the line tension $\sigma = 1.2 \pm 0.1 \times 10^{-10}$ N (see Eq. 1), using the surface tension between decane and water, $\gamma_{wo} = 48.1$ mN/m (van Buuren et al., 1993). From the coefficient c we find the intrinsic macroscopic contact angle to be $\theta_\infty = 91^\circ \pm 2^\circ$. In recent work Berg et al. (2010) state that, according to the theoretically estimated magnitude of σ, line tension only affects the contact angles of nanometer-size drops. It is the main obstacle to the experimental study of line tension. Until now (Berg et al., 2010) all experimental investigations were performed with drops that were orders of magnitude larger, and the deduced values for σ varied in sign and covered a wide range from 10^{-6} to 10^{-12} N. Our results for σ are in agreement with the majority of theoretical studies, which estimate line tension to be about 10^{-10}N (Amirfazlia and Neumann, 2004). Based on the obtained quadratic polynomial fit we can conclude that line tension changes the contact angle significantly only for decane drops with r_B smaller than 100 nm. Below that scale, the contact angle changes from $\approx 140^\circ$ (for decane drop with r_B = 2 nm) to $\approx 92^\circ$ (r_B = 100 nm). For r_B larger than 100 nm, the contact angle approaches θ_∞. Again, our results are consistent with those stated by Berg et al. (2010), that line tension plays an important role at the nanometer scale.

2.2 Decane drop on a glass surface surrounded by water

We used the same CMD procedure as described above for simulating a decane drop on glass surface surrounded by water. The only change is that the surface is glass, which here we consider to be an amorphous version of quartz. To build a glass slab we used the VMD package (Humphrey et al., 1996). The glass slab has the dimensions L_x = L_y = 17.2 nm and the same thickness as the quartz slab, i.e., 4 nm. The L_z dimensions for the system water/decane and glass were the same as for the system water/decane and quartz in previous section.

In Fig. 4 (a) we show the decane drop profile for a 8 nm diameter drop size. In this plot z is the drop height, and r is the distance of the drop interface from the z axis. For low values of z, i.e, from 0 to 20 Å, we can see that the points are scattered. This makes it difficult to fit a curve to obtain the contact angle. The scattered points in that region indicate a lack of rotational symmetry around the z axis. This is due to the amorphous condition of the glass substrate (see Fig. 4 (b)). Even on the atomic scale, glass shows surface roughness. This roughness is significant at the dimension of the simulated decane. The only way to overcome this problem using this methodology is to increase the decane drop size. But this is nearly impracticable because of computational cost. For the case of decane drops on quartz, this methodology is successful because the simulated quartz surface is almost perfectly smooth, even on the atomic scale (see Fig.4 (c)).

3 MESOSCALE MODELING OF WETTING: EFFECTS OF SURFACE ROUGHNESS

In view of our bottom-up approach, starting from Classical Molecular Dynamics and going up the length scales, we found it suitable to connect the former to a mesoscale model provided by the Lattice Boltzmann Method (LBM) (Aidun and Clausen, 2010; Chen and Doolen, 1998). This method describes a fluid as an ensemble of fictitious particles whose motion and interactions are confined to a lattice discretized in space and time. These fictitious particles

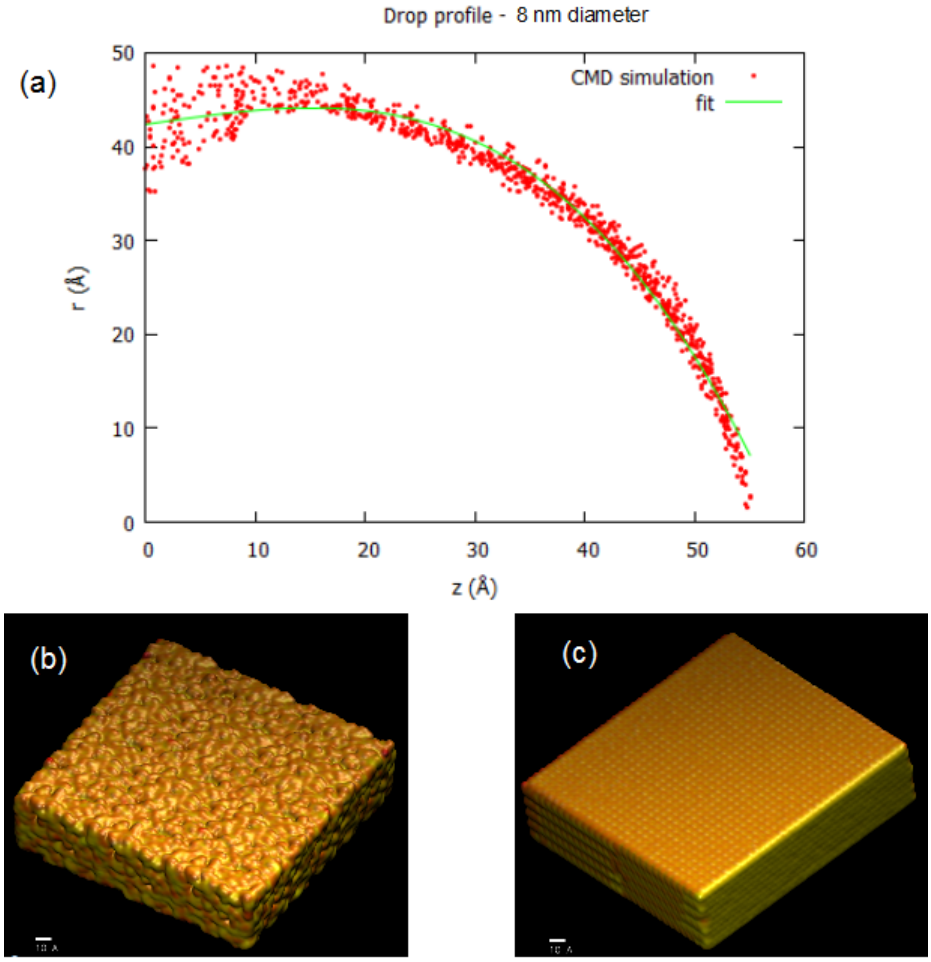

Figure 4: (a) Profile of a decane drop on a glass surface surrounded by water obtained from CMD simulations. Points represent the time averaged positions of the interfacial carbons atoms obtained from CMD simulations; the line is the cubic polynomial fit $(-0.000283z^3 + 0.00095z^2 + 0.1668z + 42.4)$**. (b) Glass and (c) quartz surfaces used in CMD simulations.**

represent not the molecules of the fluid themselves, but a collection of them with well defined hydrodynamic properties.

Although not as direct as conventional Computational Fluid Dynamics (CFD) methods (finite-element, finite-volume and finite-difference approaches), in the continuum limit the LBM yields solutions for the flow fields that match theoretical solutions of the incompressible Navier-Stokes equations. The main advantage of the LBM with respect to conventional CFD approaches is that the former deals trivially with complex boundary conditions and is highly parallelizable. In this work, we have used the Palabos implementation of the LBM algorithms, suitable for CPUs.

To analyze the effect of roughness on the contact angle, a glass surface topography obtained from Atomic Force Microscopy (AFM) measurements (see Fig. 5) was used to create a surface for LBM simulations. As the surface is relatively smooth (Fig. 5 (b)), we considered a decane drop surrounded by water on two different scales: nanometer and micrometer scales. The microscale simulation, which represents the true AFM measurement, was performed on a three-dimensional lattice of size $512\times512\times512$. To simulate nanoscale roughness, we artificially

exaggerated the vertical scale of the AFM image by multiplying it by a factor of 10. Our three-dimensional lattice in this case included $512\times512\times250$ nodes, with 250 nodes in the vertical direction. On the nanometer scale (Fig. 5 (a)) this surface shows significant roughness, which we expect to be enough to analyze its effect on the apparent contact angle. For the smooth surface, which is independent of scale, we used a $100\times100\times100$ lattice.

When scaling our surface vertically, some features at smaller scales are lost due to the resolution of our lattice. Depending on the experimental precision we are able to attain, it may be necessary to use finer grids to ensure we capture and can explain any effects of these small features. Because of the locality of the contact angle (Wolf et al., 2009), any such effects should be simulated by LBM.

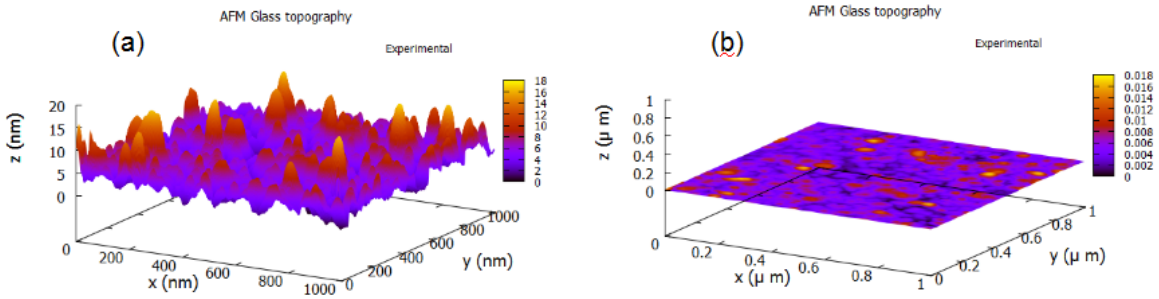

Figure 5: Atomic Force Microscopy (AFM) image of the glass topography. In (a) the glass topography is shown on the nanometer scale, and in (b) on the micrometer scale.

To describe the fluid-fluid and fluid-solid interactions in LBM simulations, we chose the standard Shan-Chen model (Shan and Chen, 1993) with BGK dynamics, and the Shan-Chen interaction parameter was varied between 1.3 and 1.4. In order to tune the solid-fluid interaction, we used the intrinsic macroscopic contact angle, $\theta_\infty = 90.6\,^\circ$, obtained from CMD simulations of a decane drop on a quartz surface surrounded by water. We accomplished this by implementing at surface nodes a fictitious bounce-back density of zero for both fluids. Although in our experimental set-up we are using a glass surface, we expect it not to affect the final results, because the difference between glass and quartz is just the arrangement of atoms (the former is amorphous and the latter is crystalline). The principal interactions based on chemical structure between solid and liquid are captured. The effect of topology should have no influence, because the length scales in the LBM simulations are orders of magnitude larger than in the CMD simulations. In a future work we will analyze the effect of this approximation.

For all simulations presented, we implemented the D3Q19 model. We used bounce-back boundary conditions at surfaces and at the edge of the simulation domain. For the BGK relaxation parameter, we chose $\Omega = 1.0$. For these preliminary studies, such as those pictured in Fig. 6, we were not concerned with maintaining the density ratio of the two fluids. At equilibrium, the density ratio was within 3% of 1 for the main phases and within 10% of 1 for the dissolved phases.

In Fig.6 (a) we show the initial condition and in (b) the steady state of a decane drop on a perfectly smooth glass surface surrounded by water. This set-up was used to tune the fluid-solid interaction in the LBM simulation. The contact angle obtained from the LBM simulation is the same as the intrinsic macroscopic contact angle from the CMD simulations, namely $\approx 90^\circ$.

After tuning the solid-fluid interaction in the Shan-Chen potential, we simulated the decane drop on a glass surface at the nanometer scale (surface referring to Fig. 5 (a)). At this scale the glass surface is rough. The results are shown in Fig. 6 (d). In this case the obtained apparent contact angle is 74.4°. We would like to stress that the apparent contact angle is measured based on the average planarity of the surface. Finally we simulated the decane drop on a glass surface at the micrometer scale (surface referring to Fig. 5 (b)). At this scale the glass surface is almost perfectly smooth. The results are shown in Fig. 6 (f).In this case the apparent contact angle is approximately 90°. As expected, once the surface roughness becomes negligible with respect to the scale of the drop, the apparent contact angle approaches the intrinsic one, which is also 90° on both the left and the right, to within the precision allowed by our lattice size. Therefore this surface is a good prototype to obtain experimentally the intrinsic contact angle on the micrometer scale.

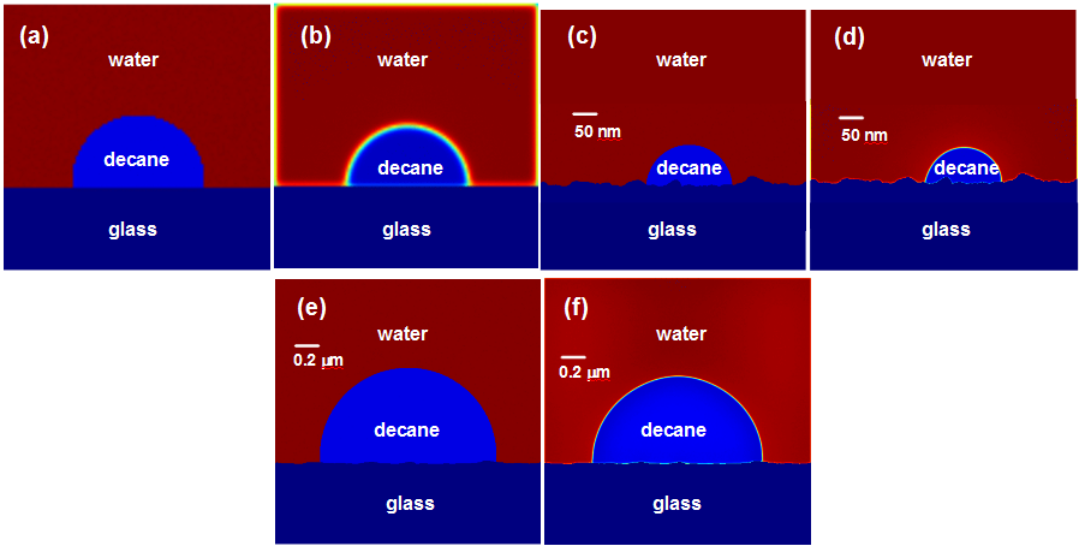

Figure 6: LBM results for a decane drop on a glass surface surrounded by water. (a) Initial condition and (b) steady state for a decane drop on a perfectly smooth surface. (c) Initial condition and (d) steady state for decane drop on a glass surface (referring to Fig. 5 (a)) at the nanometer scale (rough surface). (e) Initial condition and (f) steady state for decane drop on a glass surface (referring to Fig. 5 (b)) at the micrometer scale (almost smooth surface).

4 CONCLUSIONS

In this work we used a multi-scale modeling approach to predict the intrinsic and apparent contact angle of a decane drop on quartz/SiO_2 surfaces. For the microscopic domain, the adopted procedure using CMD simulations can in principle obtain the intrinsic micro- and macroscopic contact angles and at the same time evaluate the effect of line tension on the contact angle. This procedure, using CMD simulations, works only for almost flat surfaces, a condition satisfied for crystalline surfaces. With the intrinsic contact angle obtained from CMD simulations, the solid-fluid interaction in the Shan-Chen potential of LBM simulations was tuned. LBM simulations then deliver the apparent contact angle including the effects of roughness. This procedure is being validated by experimental studies, which will be shown in the future.

Acknowledgments

The authors wish to thank Dr. Ulisses Mello, director of IBM Research - Brazil, for support of this project and to our colleagues in the Natural Resources team for many stimulating discussions.

REFERENCES

Abraham, D. B., & Ko, L.-F., 1989. Exact derivation of the modified young equation for partial wetting. *Phys. Rev. Lett.*, vol. 63, pp. 275–278.

Aidun, C. K., & Clausen, J. R., 2010. Lattice-Boltzmann method for complex flows. *Annual Rev. Fluid Mech.*, vol. 42, pp. 439–472.

Alejandre, J., Chapela, G. A., Bresme, F., & Hansen, J.-P., 2009. The short range anion-H interaction is the driving force for crystal formation of ions in water. *J. Chem. Phys*, vol. 130, pp. 174505–174514.

Amirfazlia, A., & Neumann, A., 2004. Status of the three-phase line tension. *Advances in Colloid and Interface Science*, vol. 110, pp. 121–141.

Berg, J. K., Weber, C. M., & Riegler, H., 2010. Impact of negative line tension on the shape of nanometer-size sessile droplets. *Phys. Rev. Lett.*, vol. 3105, pp. 076103.

Brooks, B. R., 2009. Charmm: The biomolecular simulation program. *J. Comput. Chem*, vol. 30, pp. 1545–1614.

Chen, S., & Doolen, G. D., 1998. Lattice Boltzmann method for fluid flows. *Annual Rev. Fluid Mech.*, vol. 30, pp. 329–364.

Cruz-Chu, E. R., Aksimentriev, A., & Shulten, K., 2006. Water-silica force field for simulating nanodevices. *J. Phys. Chem. B*, vol. 110, pp. 21497–21508.

de Gennes, P. G., Brochard-Wyart, F., & Queré, D., 2004. *Capillarity and Wetting Phenomena: Drops, Bubbles, Pearls, Waves*. Berlin: Springer.

Fuerstenau, M. C., Jameson, G., & Yoon, R.-H., eds., 2007. *Froth flotation: a century of innovation*. Littleton, Colorado, USA: Society for Mining, Metallurgy, and Exploration.

Giovambattista, N., Debenedetti, P. G., & Rossky, P. J., 2007. Effect of Surface Polarity on Water Contact Angle and Interfacial Hydration Structure. *The Journal of Physical Chemistry B*, vol. 111, n. 32, pp 9581–9587.

Hockney, R. W., & Eastwood, J. W., eds., 1989. *Computer Simulation Using Particles*. Philadelphia: Adam Hilger.

Humphrey, W., Dalke, A., & Schulten, K., 1996. VMD – Visual Molecular Dynamics. *Journal of Molecular Graphics*, vol. 14, pp. 33–38.

Ma, M., & Hill, R. M., 2006. Superhydrophobic surfaces. *Current Opinion in Colloidal and Interface Science*, vol. 11, pp. 192–202.

Plimpton, S., 1995. Fast parallel algorithms for short range molecular dynamics. *J. Comp. Phys.*, vol. 117, pp. 1–19.

Shan, X., & Chen, H., 1993. Lattice Boltzmann model for simulating flows with multiple phases and components. *Phys. Rev. E*, vol. 47, pp. 1815.

Sergi, D., Scocchi, G., & Ortona, A., 2012. Molecular dynamics simulations of the contact angle between water droplets and graphite surfaces. *Fluid Phase Equilibria*, vol. 332, pp. 173–177.

Starov, V. M., Velarde, M. G. , & Radke, C. J., 2007. *Wetting and spreading dynamics - series: Surfactant Science*, volume 138. CRC Press, Taylor and Francis Group.

van Buuren, A. R., Marrink, S. J., & Berendsen, H. J. C., 1993. A molecular dynamics study of the decane/water interface. *J. Phys. Chem.*, vol. 97, pp. 9206–9212.

von Michaelis, H., ed., 1989. *Innovations in gold and silver recovery: phase IV*. Golden, Colorado,USA: Randol International.

Werder, T., Walther, J. H., Jaffe, R. L., Halicioglu, T., & Koumoutsakos, P., 2003. On the Water-Carbon Interaction for Use in Molecular Dynamics Simulations of Graphite and Carbon Nanotubes. *The Journal of Physical Chemistry B*, vol. 107, n.6, pp. 1345–1352.

Widom, B., 1995. Line tension and the shape of a sessile drop. *The Journal of Physical Chemistry*, vol. 99, n.9, pp. 2803–2806.

Wolf, F. G., dos Santos, L. O. E., & Philippi, P. C., 2009. Modeling and simulation of the fluid-solid interaction in wetting. *Journal of Statistical Mechanics: Theory and Experiment*, June:P06008.

Zhang, D. L., Liu, S., Puerto, M., Miller, C. A., & Hirasak, G. J., 2006. Wettability alteration and spontaneous imbibition in oil-wet carbonate formations. *Journal of Petroleum Science and Engineering*, vol. 52, pp. 213–226.